# Perceptual Contrast-Based Image Fusion: A Variational Approach

WANG Chao[1] YE Zhong-Fu[1, 2]

**Abstract** Local contrast, or variation, plays an important role in image fusion which is mainly to preserve the important information from the source images to the fusion result. Weber′s law tells us that the same variation under different backgrounds will cause different perceptual feelings, thus an ideal image processor has to take into account the effects of vision psychology and psychophysics. This paper considers the property of human visual system (HVS) and transfers the quantitative perceptual variations from each source image to the result. Using just-noticeable-difference (JND) as measurement, the multiband image′s perceptual contrast is obtained as a target. We construct a functional extremum problem to find a single band image, or fusion result, which has the closest perceptual contrast to the target one. Via the variational approach, the Euler-Lagrange equation is derived, and a gradient descent iteration is employed. Experimental results show that this method is perceptually good.

**Key words** Image fusion, variational approach, perceptual contrast, Weber′s law, human visual system (HVS), partial differential equations (PDEs)

# 1 Introduction

The purpose of image fusion is to extract and synthesize information from multiple images in order to produce a more accurate, complete and reliable composite image of the same scene or target, so that the fused image is more suitable for human or machine interpretation. It is useful for analysis, detection, recognition and tracing of targets of interest.

Image fusion can be performed in three stages, named as pixel-level, feature-level and decision-level respectively. In this paper we only discuss pixel-level image fusion, and we think all the input channels have been well registered.

Up to now, plenty of image fusion algorithms are based on multiscale decomposition, see [1] for a review. Among these decomposition methods, discrete wavelet transform (DWT) is probably the most typical one[2]. Recently, Socolinsky *et al* proposed a novel variational paradigm for image fusion, which has shown a promising future[3∼6]. In Socolinsky′s framework, variation of the intensity is the only thing to consider. However, the same variation under different backgrounds will cause different perceptions[7], as the Weber′s law tells us. The human visual system (HVS) is a necessary ingredient to be taken into consideration for all image processing tasks, including image fusion.

In the next section, the previous work will be briefly reviewed, including wavelet fusion method, Socolinsky′s method and the HVS. In Section 3, we will generalize Socolinsky′s framework by Weber′s law, present the corresponding model based on perceptual contrast, and give the discretization for the proposed scheme. The experiments are presented in Section 4. In the last section, we give some concluding remarks and the future directions for study.

# 2 Previous work and our motivation

## 2.1 Wavelet fusion framework[2]

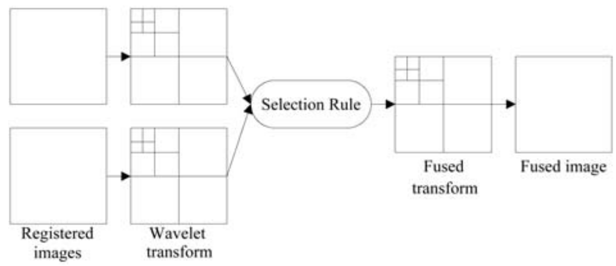


Fig. 1 DWT fusion framework[2]

Here, we will not rewrite the wavelet transform theory, but only give the existing fusion scheme based on DWT[2]. The typical diagram of DWT based image fusion can be generalized as Fig.1. The "selection rule" is the key issue of the whole task. It embodies what feature our choice is, or what we think to be the important information that should be preserved in the fused image. Different DWT-based algorithms often use different rules.

As far as the smooth component (LL) of the coarsest level DWT coefficient is concerned, Li *et al*[2] simply used the average value of each source image′s coefficients at the exact point. A maximum absolute amplitude (MAA) rule with consistency verification is used for the coefficients of the other three components (LH, HL, HH) in each level.

However, as many researchers have noticed, any nonlinear operation following DWT, such as MAA-based selection, will cause many fluctuations near the strong edges. Furthermore, with the increasing decomposition level, the fluctuations will be much more serious, and thus an insurmountable difficulty[8,9]. That greatly limits the application of DWT in image fusion.

## 2.2 Contrast-based fusion

Socolinsky *et al* have advanced a novel paradigm for image fusion. They defined the contrast (*i.e.*, the first fundamental form) of a multiband image, which agrees with the gradient definition in the special case of single band. They used the variational approach to find the solution, *i.e.*, the fused image, which has the closest gradient to the multiband′s contrast. The objective contrast (or the gradient of single-band image) is the only thing used in this framework. We do not review the procedure here, instead, we will describe the HVS-generalized contrast-based scheme in Section 3. For the detailed description of contrast fusion method, please refer to [3∼6].

Received July 13, 2005; in revised form August 10, 2006
Supported by the Graduates Innovation Fund of University of Science and Technology of China (KD2005043).
1. Institute of Statistical Signal Processing, Department of Electrical Engineering and Information Science, University of Science and Technology of China, Hefei 230027, P.R.China 2. National Laboratory of Pattern Recognition, Institute of Automation, Chinese Academy of Sciences, Beijing 100080, P.R.China
DOI: 10.1360/aas-007-0132

### 2.3 Human visual system (HVS)

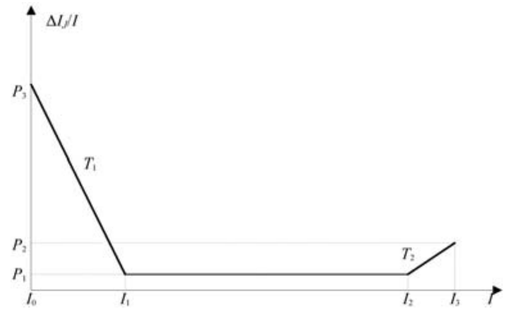

Fig. 2 The approximation of Weber′s law

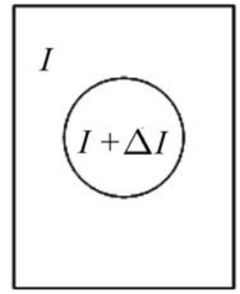

Fig. 3 Test pattern of Weber′s law

The human visual system has been already investigated for a long period of time[10~12]. Among many literatures, maybe the most important one is the Weber′s law, which says that the ratio $\Delta I_J/I$ is constant within wide limits of intensity, where $I$ is the intensity and $\Delta I_J$ is just-noticeable-difference (JND)[10,12]. According to [7], the relation between $\Delta I_J/I$ and $I$ satisfies the empirical relation in Fig.2 approximately.

Unfortunately, as stated in [13], the application of JND has some main difficulties:

• JND is only the case of the exact threshold, what the perception will be when the stimulus is high above the threshold?

• The empirical relation is obtained by the measure of physical illumination, when we utilize it in digital images, we mainly consider the intensity shown on the monitor, or printed on the paper, what is the relation between the intensity of a monitor luminance and the measure in the empirical curve?

• The curve is obtained by some simple test pattern such as Fig.3. When the natural image pattern, a complex one, is considered, what is the corresponding perception by HVS?

According to the problems listed above, in this paper, we have the following assumptions respectively:

• We do not use JND as a threshold, but we assume it to be a unit to measure the variations. A similar hypothesis has been made in [11];

• Because the gray level shown on a monitor has the identical order with the physical illumination, we think the horizontal axis ($I$) of Fig.2 is the gray level (0-255) in digital images. Following [14], we set the parameters as: $P_3 = 0.575$, $P_2 = 0.09$, $P_1 = 0.035$, $I_0 = 0$, $I_1 = 60$, $I_2 = 200$, $I_3 = 255$;

• The empirical curve still stands approximately for complex patterns.

Then according to Fig.2, we can obtain the quantitative relation between the gray level variation $\Delta I$ and perceptual variation $\Delta I_p$, measured by JND. We denote this relation as the perceptual ratio $c(I) = \Delta I_p/\Delta I$. Thus $c$ is a factor between objective intensity variation ($\Delta I$) and the perceptual one ($\Delta I_p$). Here, to avoid the zero-divided problem, $I$ is modified as $(I+1)$ in the denominators. Thus

$$\frac{\Delta I_p}{\Delta I} = c(I) \approx \begin{cases} \frac{1}{(0.575-0.009I)(I+1)}, & \text{if } 0 \le I < 60 \\ \frac{1}{0.035(I+1)}, & \text{if } 60 \le I \le 200 \\ \frac{1}{(0.035+0.001(I-200))(I+1)}, & \text{if } 200 < I \le 255 \end{cases} \quad (1)$$

This curve $c$ will be used throughout this paper.

### 2.4 Our motivation

The existing contrast-based fusion method[3~6] treats the same variation with the same importance. Because the feature in [3~6] to fuse is "contrast" (objective variation, first fundamental form, or gradient if the source is single-band), which has lost the direct current (DC) component, the intensity of the whole result is not certain, and thus some clear contrast feature in the source may be visually diminished in the result if the gray level is too high, according to Weber′s law. The Weber′s law tells us that the perceptual contrast depends not only on the variations of intensity but also on the intensity of background. We consider the DC component under the guidance of perceptual ratio $c$. We choose the perceptual contrast as the feature to fuse. Because the perceptual contrast is measured by JND, which is relevant to the local DC value, the perceptual contrast field really contains the information of DC, though in an implicit way. Thus, no matter what intensity of the whole result is, the perceptual contrast feature we want to preserve can be visually presented.

## 3 Perceptual contrast-based image fusion

The local variations play an important role in computer vision, because the human visual system is sensitive to them[7]. Image fusion is then to combine the local variation from source images to the result. However, as stated before, the same variation may cause different perceptions under different backgrounds. So in this paper, the information we want to preserve in image fusion is perceptual contrast, other than the objective variation itself. In this section, we first define the perceptual contrast of a single band image. Then, in a similar way to [3~6], we use the eigen-decomposition to define the multiband image′s perceptual contrast. Using the variational approach, we find the fused image which has the closest perceptual contrast to the multiband′s.

### 3.1 Perceptual contrast of single-band gray level image

Let $s : \Omega \to [0, 255] (\Omega \subset R^2)$ be a gray level image. Then the contrast of $s$ can be defined as its gradient $\nabla s$.

$$\boldsymbol{C}_s(x,y) = \nabla s(x,y), \qquad \forall (x,y) \in \Omega \quad (2)$$

$\boldsymbol{C}_s(x,y)$ represents the local variation of $s$ at point $(x,y)$, the magnitude of $\boldsymbol{C}_s(x,y)$ shows how fast the intensity varies, while the intensity varies fastest in the direction of $\boldsymbol{C}_s(x,y)$.

As far as the perceptual contrast is concerned, we modify $\boldsymbol{C}_s$ by the perceptual ratio $c$. The perceptual contrast $\boldsymbol{p}C_s$ can be represented as

$$\boldsymbol{p}C_s(x,y) = c(s(x,y))\nabla s(x,y), \quad \forall (x,y) \in \Omega \tag{3}$$

where curve $c$ follows (1). It can be seen that $\boldsymbol{p}C_s$ is, in some sense, the normalized variation of $s$ measured by JND.

## 3.2 Perceptual contrast of multiband image

In the case of multiband image, we combine the $\boldsymbol{p}C_s'$s of each band together, and define the multiband image's perceptual contrast.

Let $s: \Omega \to P^n, \Omega \subset R^2$ be the multiband image, where $P^n$ denotes $n$-dimensional photometric space with an arbitrary metric $g$. Let $p$ be a point in $\Omega$, and $\boldsymbol{v}$ an arbitrary unit vector in $R^2$. Let $\gamma: [-\epsilon_1, \epsilon_2] \to \Omega$ be a curve defined on a small interval, with $\epsilon_1 > 0, \epsilon_2 > 0$, such that $\gamma(0) = p$ and $\gamma'(0) = \boldsymbol{v}$. The rate of variation of $s$ at $p$ in the direction of $\boldsymbol{v}$ is given by the magnitude of the vector $\boldsymbol{s}_*(\boldsymbol{v}) \equiv \frac{d}{dl}(s \circ \gamma)(l)|_{l=0}$, where the composition operator $\circ$ denotes that $(s \circ \gamma)(l) \equiv s(\gamma(l))$, $l \in [-\epsilon_1, \epsilon_2]$. Thus we can easily get

$$\boldsymbol{s}_*(v) = J_p \boldsymbol{v} \tag{4}$$

where $J_p$ is the Jacobian matrix of $s$ at the point $p$. Then the perceptual contrast at $p$ in the direction $\boldsymbol{v}$ is given by the quantity

$$(J_p\boldsymbol{v})^t g_{s(p)}(J_p\boldsymbol{v}) = \boldsymbol{v}^t(J_p^t g_{s(p)} J_p)\boldsymbol{v} \tag{5}$$

Here, since we want to evaluate the perceptual variations, the metric $g$ should represent the perceptual meanings and we choose it as

$$g_{s(p)} = \mathrm{diag}\{c^2(s_k(p))\}_{k=1,2,\cdots n} \tag{6}$$

Let $\chi_{i,j}^2 = J_p^t g_{s(p)} J_p$, then we have

$$\chi_{i,j}^2(p) = \sum_{k=1}^{n} c^2(s_k(p)) \frac{\partial s_k}{\partial x_i}\frac{\partial s_k}{\partial x_j}, \quad 0 \le i,j \le 1 \tag{7}$$

$\chi^2$ is the image contrast form of the objective variations evaluated by a perceptual metric $g_{s(p)}$. From another viewpoint, one can think $\chi^2$ as the contrast form of perceptual variations by an Euclidean metric, since $pC_s(x,y) = c(s(x,y))\nabla s(x,y)$ stands, as defined in (3). The contrast form $\chi^2$ is the first fundamental form of the perceptual contrast of the multichannel source.

$\chi^2$ is a nonnegative matrix with two nonnegative eigenvalues $\{\lambda^+, \lambda^-\}(\lambda^+ \ge \lambda^- \ge 0)$, and the corresponding normalized eigenvectors are $\boldsymbol{E}^+, \boldsymbol{E}^-$. Then the perceptual contrast at point $p$ is defined as a 2-dimensional vector $\boldsymbol{V}^*(p)$

$$\boldsymbol{V}^*(p) = \sqrt{\lambda(p)^+} \cdot \boldsymbol{E}(p)^+ \tag{8}$$

Where $\sqrt{\lambda(p)^+}$ is the maximum perceptual variation amplitude in all 2D directions, and the corresponding variational direction is exactly $\boldsymbol{E}(p)^+$. Because $\boldsymbol{E}^+$ and $-\boldsymbol{E}^+$ can span the same eigenspace, and they do not have any priority, we must choose one out of them, or there will be a direction ambiguity. Here we select the contrast of the average bands as an auxiliary function.

$$\boldsymbol{C}_{s\_aux} = \frac{1}{n}\nabla\sum_{i=1}^{n} s_i \tag{9}$$

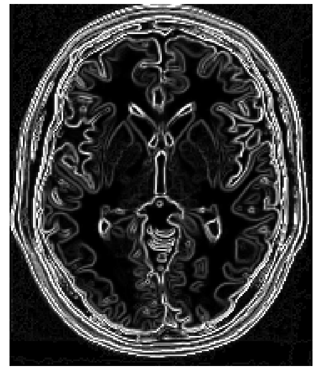

Fig. 4 Amplitude of the perceptual contrast

Because the multiband image's perceptual contrast must represent the general variations of each band, intuitively it should be close to $\boldsymbol{C}_{s\_aux}$ in direction, then a further modification to determine the value of perceptual contrast can be made as

$$\boldsymbol{V}(p) = \boldsymbol{V}^*(p)\mathrm{sign}(\boldsymbol{C}_{s\_aux}(p) \cdot \boldsymbol{V}^*(p)) \tag{10}$$

where

$$\mathrm{sign}(t) = \begin{cases} 1 & , \quad \text{if} \quad t \ge 0 \\ -1 & , \quad \text{else} \end{cases} \tag{11}$$

Equation (10) is the final definition of multiband image's perceptual contrast in this paper. For a special case $n = 1$, the single-band gray level image, we may easily find that (10) is exactly the same as (3), which shows the reasonableness of such a definition.

Here we give an example for the multiband image's perceptual contrast. The amplitude $|\boldsymbol{V}|$ of T1-, T2-weighted MRI is shown in Fig.4. According to this illustration, the main contrasts, such as the contours, in the sources are well preserved in the perceptual contrast $|\boldsymbol{V}|$.

## 3.3 Variational formulae and gradient descent

In Section 3.2, a multiband image's perceptual contrast has been constructed, which agrees with the single band's very well. It depicts the dominant perceptual variations of the sources. What to do next is how to visualize $\boldsymbol{V}(p)$. An intuitive way is to solve the equation for $f$

$$c(f(p))\nabla f(p) = \boldsymbol{V}(p), \qquad \forall p \in \Omega \tag{12}$$

However, this equation generally has no solution. The substitute is to find a 2-D function $f(p)$, $0 \le f(p) \le 255, \forall p \in \Omega$, which minimizes the following functional

$$Q^*(f) = \iint_{\Omega} |c(f)\nabla f - \boldsymbol{V}|^2 \mathrm{d}x_0 \mathrm{d}x_1 \tag{13}$$

where the notation $|\cdot|$ denotes the length of a vector.

The first fundamental form is very sensitive to noise, and so is the target perceptual contrast $\boldsymbol{V}$, since it considers only the local variation. To smooth such a noise-oriented case, TV (total variation) model[15] is employed. A very similar case has been used in image enhancement[16]. Adopt such TV energy, we minimize the following energy instead of (13).

$$Q(f) = \alpha \iint_{\Omega} |\nabla f| \mathrm{d}x_0 \mathrm{d}x_1 + \beta \iint_{\Omega} |c(f)\nabla f - \boldsymbol{V}|^2 \mathrm{d}x_0 \mathrm{d}x_1 \tag{14}$$

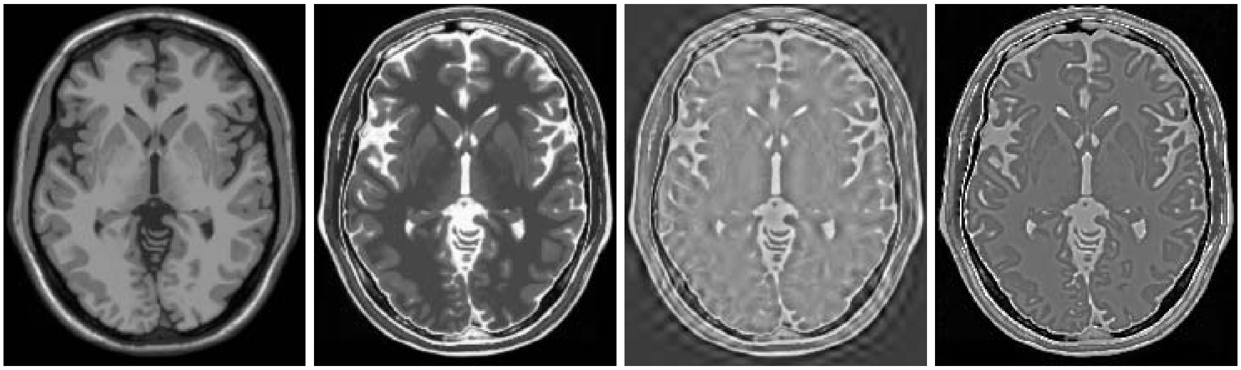

(a) MRI-T1 (b) MRI-T2 (c) DWT fusion[2] (d) Perceptual fusion

Fig. 5 Image fusion experiment on brain MRI images

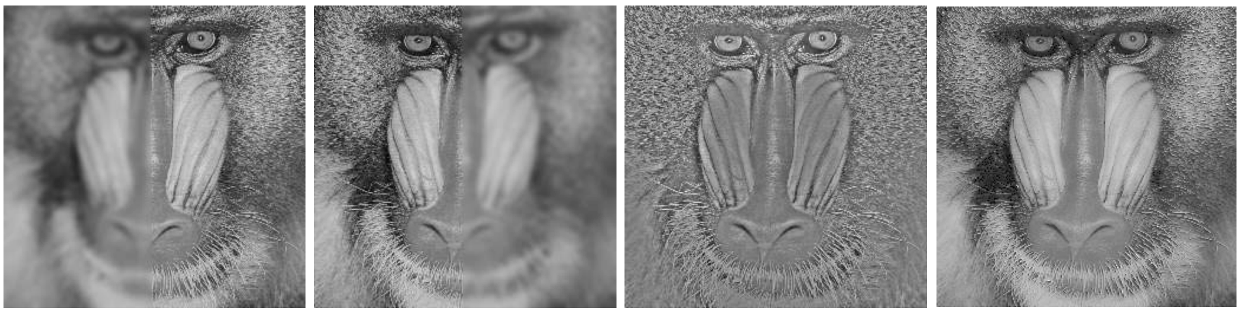

(a) Left blurred baboon (b) Right blurred baboon (c) Contrast fusion [5] (d) Perceptual fusion

Fig. 6 Image fusion experiment on "multifocused" baboon

where $\alpha, \beta$ are positive parameters weighting the smoothness and the contrast fidelity.

Using the variational approach[17], we can derive the corresponding partial differential equation (PDE) with a given Neumann boundary condition as (15).

$$\begin{cases} 2\beta(c'(f)|\nabla f|^2 + c(f)\nabla^2 f - \mathrm{div}\boldsymbol{V}) + \alpha\nabla\cdot(\frac{\nabla f}{|\nabla f|}) = 0, \mathrm{on}\,\Omega|\partial\Omega \\ \nabla f \cdot \overrightarrow{n} = 0, \mathrm{on}\ \partial\Omega \end{cases} \tag{15}$$

Here, Neumann condition is straightforward because in image processing, the boundaries are usually extended symmetrically.

Then the minimizer of (14) can be found by a gradient descent procedure with iterations like (16), where $k$ is the stepsize with a positive value. To ensure the convergence, $k$ has a small positive value in general.

$$f^{t+1} = f^t + k\cdot(2\beta(c'(f^t)|\nabla f^t|^2 + c(f^t)\nabla^2 f^t - \mathrm{div}\boldsymbol{V}) + \alpha\nabla\cdot(\frac{\nabla f^t}{|\nabla f^t|})) \tag{16}$$

Considering that curve $c$ in (1) has the finite support, (16) must be re-constrained after each iteration, as (17).

$$\begin{cases} f^{t+\frac{1}{2}} = f^t + k\cdot(2\beta(c'(f^t)|\nabla f^t|^2 + c(f^t)\nabla^2 f^t - \mathrm{div}\boldsymbol{V}) + \alpha\nabla\cdot(\frac{\nabla f^t}{|\nabla f^t|})) \\ f^{t+1} = \max(0, \min(f^{t+\frac{1}{2}}, 255)) \end{cases} \tag{17}$$

## 3.4 Discretization scheme

In this section, we discuss the issue on discretization of the iteration (17).

Because the method proposed in this paper is on pixel-level image fusion, we had better use the central difference in realizing the derivative operators to ensure their symmetric spatial support, so that the visible shift is avoided. But we do not do in such a way. Instead, we use the forward difference in all the first-order derivative operators on $f$ and $s_k$, including $\partial/\partial x_i$ in generating $\boldsymbol{V}$ and $\nabla$ in iterations; while $\boldsymbol{V}$ is concerned, "div" is realized by a backward difference. The Laplace operator $\nabla^2$ is simply realized by 5-points discretization scheme. Using these operations, we successfully avoid the computational load coming from central difference in half-pixel, and simultaneously, we ensure the absence of visible shift in pixel.

As far as the boundary region is considered, analogous to many tasks in image processing, we extend the original image ($f$ and $s_k$) symmetrically. Meanwhile, because the original image is extended symmetrically, when the "div" operator is applied, $\boldsymbol{V}$ should be extended by zero-padding.

The other parameters in (17) are chosen as: $k\beta = 0.1$, $k\alpha = 0.001$, the iteration will stop when $t$ reaches 600. In a theoretical view, $f^0$ can be any randomly selected initial value. However, the model (13) is not convex, thus we can not guarantee that the global minimum will be found using an iterative procedure of gradient descent as (17). Such an iterative procedure may seek a "good" local minimum of (14). There is reason to believe that the local extrema approach is more relevant to this image fusion task if we choose the initial value as the average of input bands, since the fusion result should represent the input bands' infor-

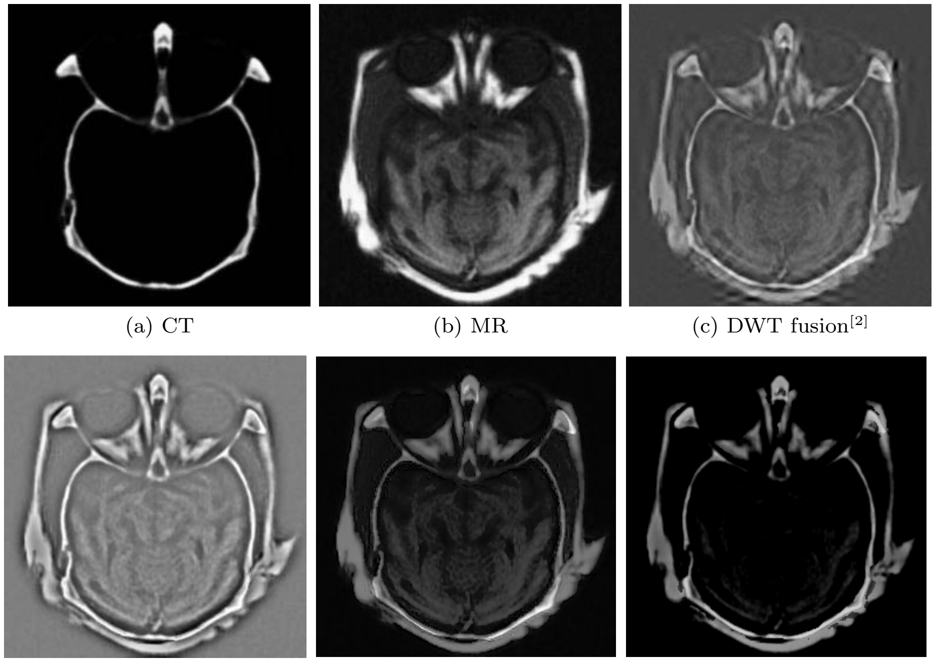

(a) CT (b) MR (c) DWT fusion[2]

(d) Contrast fusion [5] (e) Perceptual fusion (f) LPT fusion[20]

Fig. 7 Image fusion experiment on CT and MR of brain

mation, *i.e.*,

$$f^0 = \frac{1}{n}\sum_{i=1}^{n} s_i \tag{18}$$

Another key problem must be stated here. As one may find out that the curve $c$ may not be differentiable when $I = 0, 60, 200, 255$. At these points, we define $c'(0) = c'(0^+)$, $c'(60) = c'(60^+)$, $c'(200) = c'(200^-)$, $c'(255) = c'(255^-)$.

# 4 Experiments

Based on the image fusion scheme proposed above, we conduct some experiments.

First, the proposed perceptual contrast based method and DWT method[2] are compared. The source images are the brain MRI of T1-, T2-weighted[18], as shown in Figs.5(a)(b). When the method based on DWT[2] is employed, the result is Fig.5(c). It can be seen that the serious fluctuations occur around edges of the "head", and the whole image looks a little blurred. The result generated by the perceptual contrast based method looks better, as shown in Fig.5(d).

The second experiment is to compare the contrast method in [5] and the one proposed in this paper. The source images are "baboon" blurred on the left and right parts, respectively, as shown in Figs.6(a)(b). The result generated from contrast-based method in [5] is (c). The baboon′s "eyebrows" in (c) is almost mixed up with the hair on the face, and the intesity of the whole image (c) is not very satisfying, because [5] only considers the objective variations of the image with the DC component lost. For the method proposed in this paper, the result is (d), the HVS curve $c$ ensures that the same perceptual contrast stands for the same information, and under the constraint of $c$, the whole image′s gray level will not deviate too much in general.

The third experiment is also on the medical images. The source images are CT and MRI, see Figs.7(a)(b). Here we compare four methods: DWT fusion[2], contrast fusion[5], the proposed perceptual contrast fusion and Laplacian Pyramid fusion(LPT)[19], together with a subjective experiment on the four results. The results are (c)∼(f). (c) is the fusion result using DWT method in [2], where we can see the fluctuations in the region of the bottom part; (d) is the fusion result using the contrast method in [5], (e) is the result of the perceptual contrast based method, and (f) is the result of LPT[19]. The contour of MR in (e) is preserved much more clearly than in (d), and the whole intensity of (e) is more satisfying than (d), and also the details in (d) are clearer than the one in (f). In the subjective experiment, we show Fig.7 to ten judges (six of them have been working in the area of image processing or medicine, and the rest are naive), and ask them to compare each fusion result with the source images and rank them according to fusion quality. The average ranking value is listed in Table 1, which shows that the subjective experiment also supports our perceptual contrast based fusion algorithm. We also employ an objective mutual information measurement[20] to measure such results, as listed in the last two rows of Table 1. Both objective and subjective measurements show that our method is better than the other three methods.

# 5 Conclusion and future direction

In this paper, we have generalized the contrast method[3∼6] for image fusion by the characteristics of human visual system (HVS). We first define the perceptual contrast of a multiband image by eigen-decomposition, which agrees with the single band image′s well in the special case. Then we construct a functional extremum problem

Table 1 Subjective and objective ranking of the four results in Fig.7

| | DWT fusion [2] | Contrast fusion [5] | Perceptual fusion | LPT fusion [20] |
|---|---|---|---|---|
| average subjective ranking (ASR) | 2.6 | 2.4 | 1.1 | 3.9 |
| ranking of ASR | 3 | 2 | 1 | 4 |
| object measure[19] | 1.4881 | 1.2880 | 2.3201 | 0.9848 |
| ranking of object measure | 2 | 3 | 1 | 4 |

to find a single band image, which has the closest perceptual contrast to the source multiband's. Using variational approach and gradient descent, we realize the single band visualization of the target perceptual contrast via iterations. Experimental results show that this perceptual contrast based method is perceptually good.

However, in the method proposed in this paper, there are still some problems. They mainly correspond to the assumptions listed in the last of Section 2.

- JND is actually not the unit measure of variations, *i.e.*, the perceptual contrast is not linear with JND when the stimulus is high above the JND, though some researchers have done so. A more reasonable perceptual measure might be used for this model.
- Since the test patterns for HVS are simple, under complex circumstance, we can find some other manner to use the HVS, *e.g.*, can the background intensity $I$ be used by the local blurred intensity?
- In general, multiscale methods have better performance than the single scale one, under the same other conditions. How to incorporate multiscale schemes into the perceptual contrast framework (*e.g.*, in [21]) is also a further topic to study.

These problems deserve our further study.

## References

1 Zhang Z, Blum R S. A categorization of multiscale-decomposition-based image fusion schemes with a performance study for a digital camera application. *Proceedings of the IEEE*, 1999, **87**(8): 1315∼1326

2 Li H, Manjunath B S, Mitra S K. Multisensor image fusion using the wavelet transform. *Graphical Models and Image Processing*, 1995, **57**(3): 235∼245

3 Socolinsky D A, Wolff L B. Multispectral image visualization through first-order fusion. *IEEE Transactions on Image Processing*, 2002, **11**(8): 923∼931

4 Socolinsky D A, Wolff L B. A new visualization paradigm for multispectral imagery and datafusion. In: Proceedings of IEEE Conference on Computer Vision and Pattern Recognition, IEEE, 1999: **1**: 319∼324

5 Socolinsky D A. Dynamic range constraints in image fusion and visualization. In: Proceedings of Signal and Image Processing 2000, 349∼354

6 Socolinsky D A. A Variational Approach to Image Fusion. [Ph. D. Dissertation], The Johns Hopkins University, 2000

7 Pratt W K. *Digital Image Processing*, 2nd Ed., New York: John Wiley, 1991

8 Starck J L, Candès E J, Donoho D L. The Curvelet Transform for Image Denoising. *IEEE Transactions on Image Processing*, 2002, **11**(6): 670∼684

9 Petrović V S, Xydeas C S. Gradient-Based Multiresolution Image Fusion. *IEEE Transactions on Image Processing*, 2004, **13**(2): 228∼237

10 Hecht S. The Visual Discrimination of Intensity and the Weber-Fechner Law. *The Jounal of General Physiology*, 1924, **7**: 235∼267

11 Xie Z, Stockham T G Jr. Toward the Unification of Three Visual Laws and Two Visual Models in Brightness Perception. *IEEE Transactions on Systems, Man, and Cybernetics*, 1989, **19**(2): 379∼387

12 Weber E H. *De pulsu, resorptine, auditu et tactu*, Annotationes anatomicae et physiologicae, 1834

13 Wang Z, Bovik A C, Sheikh H R, Simoncelli E P. Image Quality Assesment: From Error Visibility to Structual Similarity. *IEEE Transactions on Image Processing*, 2004, **13**(4): 600∼612

14 Ma K K, Huang L. Perceptually Based Subband AMBTC Image Coder. In: Proceedings of International Conference on Information, Communication and Signal Processing, 1997, IEEE, **1**: 505∼509

15 Rudin L, Osher S, Fatemi E. Nonlinear total variation based noise removal algorithms. *Physica D*, 1992, **60**: 259∼268

16 Wang C, Ye Z F. Variational Enhancement for Infrared Images. *Journal of Infrared and Millimeter Waves*, 2006, **25**(4): 306∼310

17 Xu J, Gui Z. *Variational Approach*, Tongji University Press, Shanghai, China, 1999

18 BrainWeb: Simulated Brain Database. [Online], available: http://www.bic.mni.mcgill.ca/brainweb/, March, 2004

19 Burt P J, Adelson E H. The Laplacian Pyramid as a Compact Image Code. *IEEE Transactions on Communications*, 1983, **31**(4): 532∼540

20 Qu G H, Zhang D L, Yan P F. Infomation measure for performance of image fusion. *Electronics Letters*, 2002, **38**(7): 313∼315

21 Scheunders P, Backer S D. Multispectral image fusion fusion and merging using multiscale fundamental forms. In: Proceedings of IEEE International Conference on Image Processing, 2001: 902∼905

**WANG Chao** Received his B. E. degree on electrical and information engineering, from University of Science and Technology of China (USTC) in 2002. He is a Ph.D. candidate on signal and information processing at USTC. His research interests include image processing and coding, *etc.* Corresponding author of this paper. E-mail: chaowang@mail.ustc.edu.cn

**YE Zhong-Fu** Received his Ph. D. degree from University of Science and Technology of China (USTC)in 1998. He is a professor at Department of Electronic Engineering and Information Science, USTC. His research interests include image processing, radar and communication signal processing. E-mail: yezf@ustc.edu.cn